

Kinetic and Spectroscopic Studies of the ATP:Corrinoid Adenosyltransferase PduO from *Lactobacillus reuteri*: Substrate Specificity and Insights into the Mechanism of Co(II)corrinoid Reduction[†]

Kiyoung Park,[‡] Paola E. Mera,[§] Jorge C. Escalante-Semerena,[§] and Thomas C. Brunold^{*,‡}

Department of Chemistry, University of Wisconsin—Madison, Madison, Wisconsin 53706, and Department of Bacteriology, University of Wisconsin—Madison, Madison, Wisconsin 53706

Received March 11, 2008; Revised Manuscript Received May 31, 2008

ABSTRACT: The PduO-type ATP:corrinoid adenosyltransferase from *Lactobacillus reuteri* (*LrPduO*) catalyzes the formation of the essential Co–C bond of adenosylcobalamin (coenzyme B₁₂) by transferring the adenosyl group from cosubstrate ATP to a transient Co¹⁺corrinoid species generated in the enzyme active site. While PduO-type enzymes have previously been believed to be capable of adenosylating only Co¹⁺cobalamin (Co¹⁺Cbl[−]), our kinetic data obtained in this study provide in vitro evidence that *LrPduO* can in fact also utilize the incomplete corrinoid Co¹⁺cobinamide (Co¹⁺Cbi) as an alternative substrate. To explore the mechanism by which *LrPduO* overcomes the thermodynamically challenging reduction of its Co²⁺corrinoid substrates, we have examined how the enzyme active site alters the geometric and electronic properties of Co²⁺Cbl and Co²⁺Cbi⁺ by using electronic absorption, magnetic circular dichroism, and electron paramagnetic resonance spectroscopic techniques. Our data reveal that upon binding to *LrPduO* that was preincubated with ATP, both Co²⁺corrinoids undergo a partial (~40–50%) conversion to distinct paramagnetic Co²⁺ species. The spectroscopic signatures of these species are consistent with essentially four-coordinate, square-planar Co²⁺ complexes, based on a comparison with the results obtained in our previous studies of related enzymes. Consequently, it appears that the general strategy employed by adenosyltransferases for effecting Co²⁺ → Co¹⁺ reduction involves the formation of an “activated” Co²⁺corrinoid intermediate that lacks any significant axial bonding interactions, to stabilize the redox-active, Co 3d_{z²}-based molecular orbital.

Coenzyme B₁₂, which is also known as adenosylcobalamin (AdoCbl),¹ provides one of very few known examples of a bio-organometallic species (*1*). AdoCbl contains a cobalt(III) ion that is equatorially ligated by four nitrogens of a tetrapyrrole macrocycle, termed the corrin ring, and axially coordinated by the 5′-carbon atom of an adenosyl (Ado) moiety on the “upper” face and a nitrogen atom from 5,6-dimethylimidazole (DMB) on the “lower” face (Figure 1) (*2*). The DMB is part of a nucleotide loop that is tethered to the corrin ring at C¹⁷; in adeonsylcobinamide (AdoCbi⁺), this loop is absent and the lower axial coordination site is occupied by a water molecule to complete a distorted octahedral ligand environment of the Co³⁺ ion (*3*).

AdoCbl serves as a cofactor for numerous distinct enzymes that catalyze radical-induced rearrangement reactions (*4–10*), such as methylmalonyl-CoA mutase, glutamate mutase, diol dehydratase, and ethanolamine ammonia lyase, or ribonucleotide reduction, as exemplified by the ribonucleotide triphosphate reductase (*11*). Common to these enzymes is the fact that the first step in their respective catalytic cycles involves homolytic cleavage of the cofactor’s Co–C bond to yield Co²⁺cobalamin (Co²⁺Cbl) and an organic radical centered on the 5′-carbon of the Ado moiety. The Ado• radical generated in this process then abstracts a hydrogen atom from substrate to initiate a protein-mediated rearrangement reaction that eventually leads to product formation and regeneration of the AdoCbl cofactor (*12–14*).

Eukaryotes lack the biosynthetic machinery needed to synthesize AdoCbl de novo. Instead, those eukaryotes that utilize AdoCbl in their metabolism (which does not include plants) convert exogenous cobalamins, such as vitamin B₁₂ (in which the upper axial coordination site is occupied by a CN[−] moiety rather than Ado), to AdoCbl by using a class of enzymes termed adenosyltransferases (*15, 16*). The importance of these enzymes is highlighted by the fact that the malfunctioning of the human adenosyltransferase (hATR) can cause methylmalonic aciduria, an autosomal disorder that is often fatal in infants (*17*). Many prokaryotes also require AdoCbl, e.g., for the utilization of propionediol and ethanol-

[†] This work was supported in part by National Science Foundation Grant MCB-0238530 (to T.C.B.) and National Institutes of Health Grant R01-GM40313 (to J.C.E.-S.). P.E.M. was supported in part by NIH NRSA F31-GM081979.

* To whom correspondence should be addressed: Department of Chemistry, 1101 University Ave., Madison, WI 53706. Phone: (608) 265-9056. Fax: (608) 262-6143. E-mail: brunold@chem.wisc.edu.

[‡] Department of Chemistry.

[§] Department of Bacteriology.

¹ Abbreviations: Abs, electronic absorption; AdoCbl, adenosylcobalamin; AdoCbi⁺, adenosylcobinamide; H₂OCbl⁺, aquacobalamin; Cbl, cobalamin; cbi, cobinamide; CNCbl, cyanocobalamin; (H₂O)₂Cbi²⁺, diaquacobinamide; (CN)₂Cbi, dicyanocobinamide; DMB, dimethylbenzimidazole; EPR, electron paramagnetic resonance; hATR, human adenosyltransferase; *LrPduO*, *Lactobacillus reuteri* PduO; MCD, magnetic circular dichroism; NaBH₄, sodium borohydride.

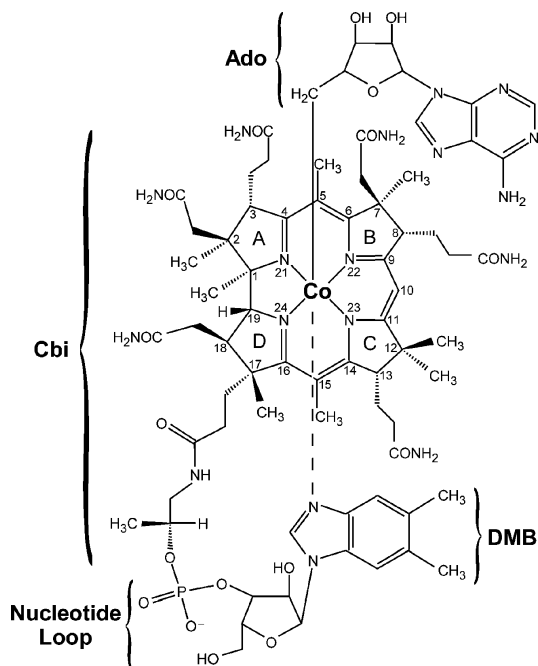


FIGURE 1: Schematic representation of the adenosylcobalamin cofactor (AdoCbl). In adenosylcobinamide (AdoCbi⁺), the nucleotide loop including the DMB base is absent and a water molecule occupies the lower axial position.

amine to produce substrates for ATP production and as sources of carbon and nitrogen, respectively (7, 8). Some of these organisms are capable of synthesizing AdoCbl de novo in a process involving more than 25 enzymes, which catalyze the stepwise conversion of 5-aminolevulinic acid to the complete cofactor via an intermediate named cobyrinic acid, a cobalamin precursor that possesses all of the necessary functionality except for the nucleotide loop and the axial Ado ligand (18).

Regardless of whether an organism synthesizes AdoCbl de novo or salvages incomplete corrinoids from its environment, both processes require two one-electron reduction steps to convert Co³⁺ to Co¹⁺ and the formation of the essential Co–C bond by transferring the Ado group from a molecule of ATP to the transiently formed Co¹⁺corrinoid species (19, 20). While previous studies revealed that the Co^{3+/2+}corrinoid reduction potential is sufficiently positive to ensure that the Co³⁺corrinoid is converted to the Co²⁺ state in the reducing environment of the cytoplasm (21), the Co^{2+/1+}corrinoid potential is lower than the midpoint potentials of putative *in vivo* reducing agents. For example, the Co^{2+/1+} reduction potential of aqueous Co²⁺Cbl ($E^\circ = -610$ mV) is well below that of the semiquinone/reduced flavin couple of flavodoxin A (FldA; $E^\circ = -440$ mV) (22, 24). Despite this apparent thermodynamic dilemma, it has been shown that in the presence of adenosyltransferases, the Co²⁺ → Co¹⁺ reduction can be effected under physiologically relevant conditions (25–27).

Previously, our spectroscopic and computational studies of two representative members of the family of adenosyltransferases, CobA from *Salmonella enterica* and hATR, have provided definitive clues about how these enzymes overcome the thermodynamically challenging task of reducing Co²⁺corrinoids to their Co¹⁺ oxidation state (28, 29). Specifically, we have shown that upon binding of Co²⁺cobinamide (Co²⁺Cbi⁺) to CobA complexed with co-

substrate ATP, the axially bound water molecule (partially) dissociates to generate an effectively four-coordinate square-planar Co²⁺ species. As a result of this (partial) ligand dissociation, the redox-active Co 3d_{z²} orbital that is oriented toward the axial coordination sites is significantly stabilized in energy, thereby increasing the Co^{2+/1+} reduction midpoint potential by an estimated 250 mV (28). Remarkably, the same spectroscopic signatures characterizing this “activated” four-coordinate Co²⁺ species features have been found to develop upon binding of Co²⁺Cbl to hATR in the presence of ATP (29), even though hATR and CobA are structurally and evolutionarily unrelated (7, 30, 31).

Recently, St. Maurice et al. (32) purified an hATR-type adenosyltransferase from *Lactobacillus reuteri*, termed *LrPduO*, and reported its X-ray crystal structure with ATP bound to the active site. *In vivo* and *in vitro* experiments have confirmed that *LrPduO* can convert Co¹⁺Cbl[−] to AdoCbl and revealed that it can substitute for CobA in *Salmonella enterica*, implying that *LrPduO* possesses the ability to adenosylate both Co²⁺Cbl and Co²⁺Cbi⁺ (16, 32). In this study, we have performed a detailed kinetic and spectroscopic characterization of *LrPduO* to obtain molecular-level insight into certain steps of the catalytic mechanism employed by this enzyme. Our kinetic parameters obtained for the reaction of Co¹⁺Cbi with *LrPduO*/ATP confirm that cobinamide can serve as an alternative substrate for this adenosyltransferase, while our spectroscopic data indicate that *LrPduO* utilizes the same general strategy for promoting Co²⁺ → Co¹⁺ reduction as CobA and hATR, namely, generating an effectively four-coordinate Co²⁺corrinoid species regardless of whether Co²⁺Cbl or Co²⁺Cbi⁺ is used as the substrate. Nonetheless, a comparison of the results obtained for *LrPduO* and those reported previously for hATR and CobA reveals small but notable differences with regard to the substrate specificity and degree of Co²⁺corrinoid activation.

MATERIALS AND METHODS

Cofactors and Chemicals. Aquacobalamin (H₂OCbl⁺), dicyanocobinamide [(CN)₂Cbi], and sodium borohydride (NaBH₄) were purchased from Sigma and used as obtained. Diaquacobinamide [(H₂O)₂Cbi²⁺] was prepared by reducing (CN)₂Cbi with NaBH₄, loading the reaction mixture on a C18 SepPack column, washing with doubly distilled H₂O, and eluting the product with methanol, as described in a previous report (28). Co²⁺Cbl and Co²⁺Cbi⁺ were prepared by adding NaBH₄ to degassed aqueous solutions of H₂OCbl⁺ and (H₂O)₂Cbi²⁺, respectively, in the presence of 60% (v/v) glycerol, and the progress of the conversion was monitored spectrophotometrically.

Protein Production and Purification. Recombinant PduO protein from *L. reuteri* was obtained by overexpressing a pTEV3 plasmid transformed into *Escherichia coli* strain BL21(DE3). pTEV3 encodes the *LrPduO* protein with an N-terminal His₆ tag (32, 33). This His₆ tag was subsequently clipped off using rTEV protease, and the tag-free enzyme was purified using a HisTrap FF column (Amersham Biosciences), as described previously (32). Purified *LrPduO* was stored at −80 °C in Tris-HCl buffer (0.1 M, pH 8 at 4 °C) containing NaCl (0.5 M). Protein samples used for kinetic analyses additionally contained 10% (v/v) glycerol.

Table 1: Kinetic Parameters for the *Lr*PduO-Catalyzed Conversion of $\text{Co}^{1+}\text{Cbl}^-$ and Co^{1+}Cbi to AdoCbl and AdoCbi^+ , Respectively^a

substrate	k_{cat} (s^{-1})	K_{m} (μM)	$k_{\text{cat}}/K_{\text{m}}$ ($\text{M}^{-1} \text{s}^{-1}$)
$\text{Co}^{1+}\text{Cbl}^-$	$(2.4 \pm 0.1) \times 10^{-2}$	$(13 \pm 1) \times 10^{-2}$	$(1.8 \pm 0.2) \times 10^5$
Co^{1+}Cbi	$(2.0 \pm 0.2) \times 10^{-2}$	$(9.6 \pm 1.4) \times 10^{-2}$	$(2.1 \pm 0.4) \times 10^5$

^a Data for $\text{Co}^{1+}\text{Cbl}^-$ were taken from ref 32.

Kinetic Studies. Activity assays were performed as described previously (32) without modifications (final *Lr*PduO concentration of 1 $\mu\text{g}/\text{mL}$). AdoCbi^+ formation was monitored spectrophotometrically at 388 nm, which corresponds to the peak position of the dominant absorption feature of Co^{1+}Cbi . The values of V_{max} and K_{m} were determined from plots of the initial velocity versus substrate concentration. All kinetic parameters were determined in duplicate; their values and uncertainties as reported in this paper correspond to the average of the two measurements and their standard deviations, respectively.

Sample Preparation. Solutions of *Lr*PduO [in 50 mM Tris-HCl buffer (pH 8) containing 0.5 M NaCl] in the absence or presence of 3 mM MgATP were purged separately with Ar gas for 30 min at 4 °C before they were combined with the degassed free Co^{2+} corrinoid solutions in a 0.9:1.0 Co^{2+} corrinoid:*Lr*PduO molar ratio in a sealed anaerobic vial (final enzyme concentration of 0.4 mM). The reaction mixtures, which contained 60% (v/v) glycerol, were then transferred anaerobically into the appropriate sample cells (previously purged with Ar gas) and immediately frozen in liquid N_2 .

Spectroscopy. Low-temperature electronic absorption (Abs) and magnetic circular dichroism (MCD) spectra were collected on a Jasco J-715 spectropolarimeter in conjunction with an Oxford Instruments SM-4000 8T magnetocryostat. All MCD spectra presented in this paper were recorded by taking the difference between spectra collected with the magnetic field oriented parallel and antiparallel to the light propagation axis to remove contributions from the natural CD and glass strain.

X-Band EPR spectra were obtained by using a Bruker ESP 300E spectrometer in conjunction with an Oxford ESR 900 continuous-flow liquid helium cryostat and an Oxford ITC4 temperature controller. The microwave frequency was measured with a Varian EIP model 625A CW frequency counter. All spectra were collected using a modulation amplitude of 10 G, a modulation frequency of 100 kHz, and a time constant of 41 ms. EPR spectral simulations were performed using the WEPR program developed by F. Neese (34).

RESULTS AND ANALYSIS

Kinetic Studies. To explore whether *Lr*PduO possesses the ability to adenosylate incompletely assembled corrinoids in addition to $\text{Co}^{1+}\text{Cbl}^-$ (32), initial velocity kinetic measurements were performed using chemically reduced Co^{1+}Cbi as the substrate. In these experiments, the concentration of Co^{1+}Cbi was varied while that of the cosubstrate ATP was kept at saturation. The apparent K_{m} for Co^{1+}Cbi (0.096 μM) was found to be similar to the one reported for $\text{Co}^{1+}\text{Cbl}^-$ (0.13 μM). Likewise, the rates at which *Lr*PduO can adenosylate $\text{Co}^{1+}\text{Cbl}^-$ and Co^{1+}Cbi are nearly indistinguishable ($k_{\text{cat}} = 2.0$ and $2.4 \times 10^{-2} \text{ s}^{-1}$, respectively; see Table 1), indicating that, at least in vitro, the nucleotide loop is

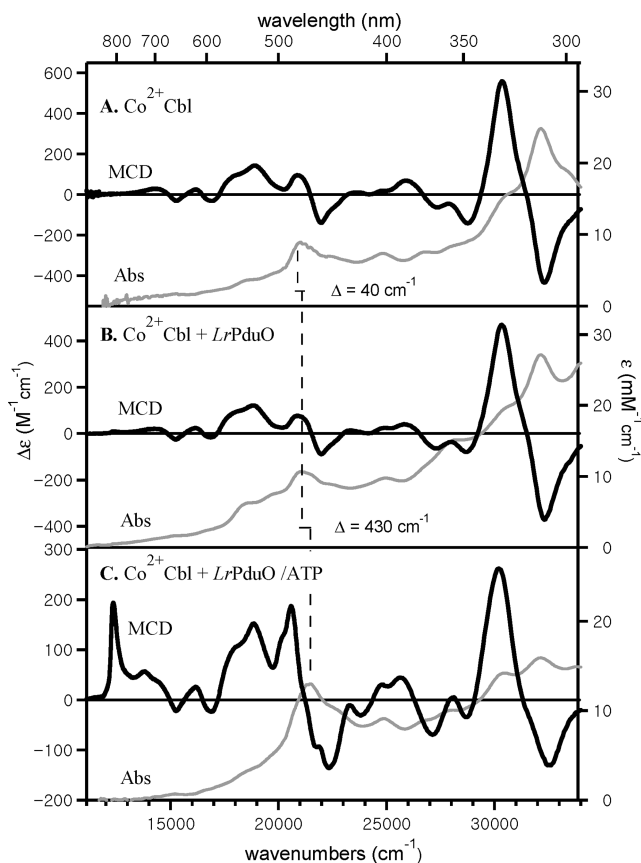


FIGURE 2: Abs (gray traces, right axis) and 7 T MCD (black traces, left axis) spectra collected at 4.5 K of (A) free Co^{2+}Cbl , (B) Co^{2+}Cbl in the presence of *Lr*PduO, and (C) Co^{2+}Cbl in the presence of the *Lr*PduO/ATP complex. The peak position of the dominant Abs feature (the α -band) is indicated by the solid vertical line.

not required for the binding and adenosylation of the corrinoid substrate by *Lr*PduO.

$\text{Co}^{2+}\text{Cbl} \leftrightarrow \text{LrPduO}$ Interactions. (A) $\text{Co}^{2+}\text{Cbl} + \text{LrPduO}$. The low-temperature Abs spectra of Co^{2+}Cbl in the absence and presence of *Lr*PduO are nearly identical with respect to band positions and intensities (cf. panels A and B of Figure 2). Although the addition of *Lr*PduO causes a minor blue shift of the prominent feature in the visible spectral region [the α -band (35)] of the Co^{2+}Cbl Abs spectrum, from 21010 to 21050 cm^{-1} (Table 2), it has no discernible effect on the position of the dominant Abs feature in the near-UV region at $\sim 32150 \text{ cm}^{-1}$ (note that the shoulder near 18520 cm^{-1} in the $\text{Co}^{2+}\text{Cbl} + \text{LrPduO}$ Abs spectrum is due to the presence of a small fraction of reoxidized corrinoid in that sample).

A complementary and considerably more sensitive probe of the interaction between Co^{2+}Cbl and *Lr*PduO is provided by low-temperature MCD spectroscopy. Because the low-energy region of the Co^{2+} corrinoid MCD spectra is dominated by ligand-field (LF) transitions, this region is particularly valuable for monitoring changes in the Co^{2+} coordination environment (35). Hence, the fact that the MCD spectra of

Table 2: Changes in the α -Band Positions of Co^{2+}Cbl and $\text{Co}^{2+}\text{Cbi}^+$ Caused by the Addition of *LrPduO* in the Absence and Presence of Cosubstrate ATP, As Determined from the 4.5 K Abs Spectra in Figures 2 and 4^a

species	free corrinoid	corrinoid with <i>LrPduO</i>	corrinoid with <i>LrPduO</i> /ATP
Co^{2+}Cbl	21010 cm^{-1} (476.0 nm)	21050 cm^{-1} (475.0 nm)	21480 cm^{-1} (465.5 nm)
$\text{Co}^{2+}\text{Cbi}^+$	21250 cm^{-1} (470.5 nm)	21250 cm^{-1} (470.5 nm)	21480 cm^{-1} (465.5 nm)

^a Note that a blue shift of the α -band reflects a weakening of the axial ligand– Co^{2+} –corrinoid bonding interaction.

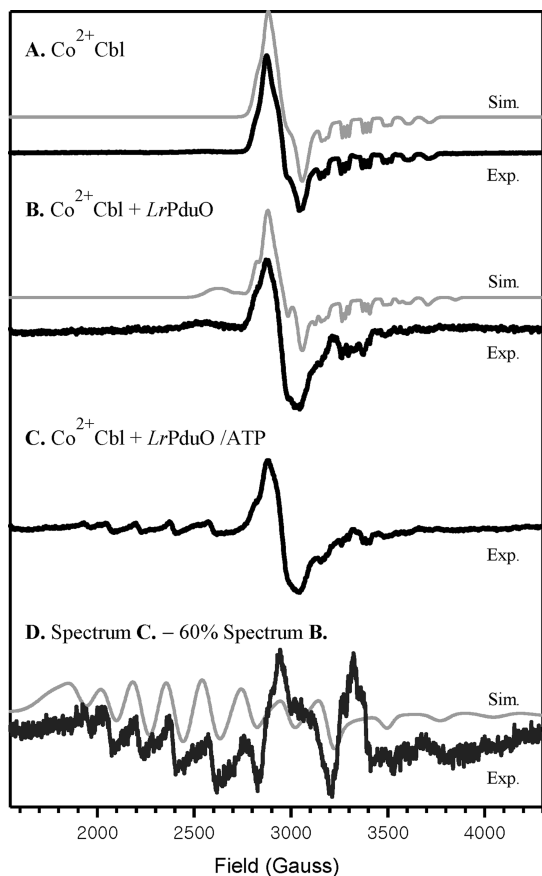


FIGURE 3: EPR spectra collected at 20 K of (A) free Co^{2+}Cbl , (B) Co^{2+}Cbl in the presence of *LrPduO*, and (C) Co^{2+}Cbl in the presence of the *LrPduO*/ATP complex. Spectrum D was obtained by subtracting 60% of spectrum B from spectrum C. Spectral simulations (thin lines) were performed using the parameters provided in Table 3.

Co^{2+}Cbl in the absence and presence of *LrPduO* are virtually identical (cf. panels A and B of Figure 2) rules out any major structural perturbations to the Co^{2+} center upon cofactor binding to the enzyme active site.

Consistent with our MCD results, the EPR spectra of Co^{2+}Cbl in the absence and presence of *LrPduO* are nearly superimposable (cf. panels A and B of Figure 3). However, closer examination of the EPR spectrum of $\text{Co}^{2+}\text{Cbl} + \text{LrPduO}$ reveals the presence of a broad feature near 2600 G that has no counterpart in the spectrum of the free cofactor. This feature is characteristic of base-off Co^{2+}Cbl (36, 37), a species in which a water molecule binds to the lower axial coordination site of the Co^{2+} center that was originally occupied by the DMB moiety in base-on Co^{2+}Cbl (Figure 1). A quantitative analysis of the $\text{Co}^{2+}\text{Cbl} + \text{LrPduO}$ EPR spectrum reveals that this sample contains $\sim 30\%$ base-off Co^{2+}Cbl . This finding correlates nicely with the slight blue shift of the α -band that is observed in the Co^{2+}Cbl Abs spectrum upon addition of *LrPduO* (panels A and B of Figure 2 and Table 2). The g and ^{59}Co hyperfine $A(\text{Co})$ values

obtained from simulations of the EPR spectra presented in Figure 3 are summarized in Table 3.

(B) $\text{Co}^{2+}\text{Cbl} + \text{LrPduO}/\text{ATP}$. While the spectral changes in response to Co^{2+}Cbl binding to substrate-free *LrPduO* are quite modest (see above), a rather significant blue shift of the α -band is observed in the Abs spectrum of Co^{2+}Cbl upon addition of the *LrPduO* complexed with the cosubstrate ATP (cf. panels B and C of Figure 2 and Table 2). This shift occurs in parallel with a dramatic change to the MCD spectrum, most notably the appearance of new features at ~ 12340 and 20580 cm^{-1} (Figure 2C). Because the MCD feature at 12340 cm^{-1} has no discernible counterpart in the Abs spectrum, it can be attributed to a magnetic dipole-allowed $\text{Co}^{2+} d \rightarrow d$ transition (38, 39). An analogous low-energy MCD feature has been observed for Co^{2+}Cbl bound to the hATR/ATP complex, where it was shown to reflect the presence of an effectively four-coordinate Co^{2+}Cbl species (29). Our MCD data thus provide compelling evidence that a four-coordinate Co^{2+}Cbl species is also formed when Co^{2+}Cbl binds to the *LrPduO*/ATP complex. This conversion is not complete, however, as the negative features at 15250 and 16880 cm^{-1} and the positive features at 18000 and 18850 cm^{-1} in the MCD spectrum of $\text{Co}^{2+}\text{Cbl} + \text{LrPduO}/\text{ATP}$ (Figure 2C) are characteristic of base-on Co^{2+}Cbl (see Figure 2A). This fraction of five-coordinate Co^{2+}Cbl corresponds to either an unbound corrinoid substrate or an enzyme-bound species that has resisted conversion to the four-coordinate form.

In agreement with our MCD data presented in Figure 2, the EPR spectrum of $\text{Co}^{2+}\text{Cbl} + \text{LrPduO}/\text{ATP}$ (Figure 3C) reveals the presence of at least two distinct paramagnetic species, one exhibiting an EPR spectrum characteristic of base-on Co^{2+}Cbl (see Figure 3A) and the other giving rise to the appearance of a series of widely spread resonances in the low-field region. To better resolve the features associated with the latter species, the suitably scaled ($\times 0.6$) $\text{Co}^{2+}\text{Cbl} + \text{LrPduO}$ EPR spectrum (Figure 3B) was subtracted from the composite spectrum in Figure 3C to yield the trace shown in Figure 3D. As expected on the basis of our MCD data analysis (vide supra), the resulting spectrum is very similar to that reported for the four-coordinate Co^{2+}Cbl species in samples of Co^{2+}Cbl and the hATR/ATP complex (29). In particular, the g_2 , g_3 , and $A(\text{Co})$ values obtained from a fit of the EPR spectrum in Figure 3D are much larger than those of any five-coordinate Co^{2+}Cbl species (Table 3) and are instead characteristic of an essentially square-planar Co^{2+} complex that lacks any significant axial bonding interactions (28, 40, 41).

$\text{Co}^{2+}\text{Cbi}^+ \leftrightarrow \text{LrPduO}$ Interactions. (A) $\text{Co}^{2+}\text{Cbi}^+ + \text{LrPduO}$. The low-temperature Abs and MCD spectra of $\text{Co}^{2+}\text{Cbi}^+$ in the absence and presence of *LrPduO* are very similar to each other (cf. panels A and B of Figure 4). However, while the addition of *LrPduO* to the $\text{Co}^{2+}\text{Cbi}^+$ solution has no effect on the peak position of the α -band

Table 3: EPR g Values and ^{59}Co Hyperfine Values $A(\text{Co})$ (in megahertz) from the Spectral Simulations Presented in Figures 3 and 5

species	spectrum ^a	g_1	g_2	g_3	$A_1(\text{Co})$	$A_2(\text{Co})$	$A_3(\text{Co})$
free $\text{Co}^{2+}\text{Cbl}^b$	3A	2.00	2.23	2.28	305	30	40
$\text{Co}^{2+}\text{Cbl} + \text{LrPduO}^c$	3B	2.00	2.23	2.28	305	30	40
		2.00	2.34	2.37	400	220	220
$\text{Co}^{2+}\text{Cbl} + \text{LrPduO}/\text{ATP}$	3D	1.99	2.70	2.72	770	755	595
free $\text{Co}^{2+}\text{Cbi}^{+b}$	5A	2.00	2.34	2.34	405	220	220
$\text{Co}^{2+}\text{Cbi}^{+} + \text{LrPduO}$	5B	2.00	2.34	2.37	400	220	220
$\text{Co}^{2+}\text{Cbi}^{+} + \text{LrPduO}/\text{ATP}$	5D	1.99	2.65	2.74	810	665	565

^a The labels refer to the spectra in Figures 3 and 5. ^b From ref 28. ^c This spectrum has contributions from ~70% base-on and ~30% base-off Co^{2+}Cbl .

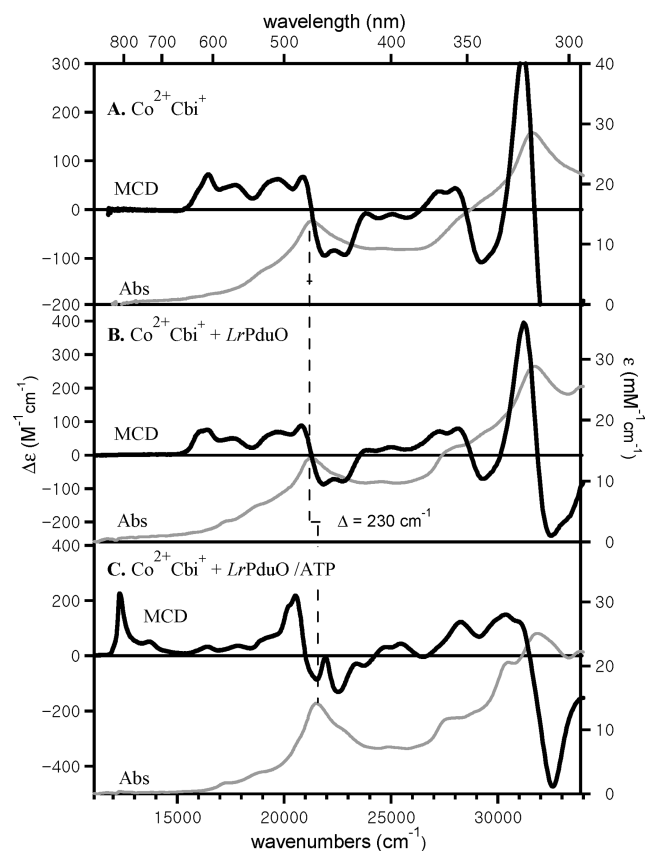


FIGURE 4: Abs (gray traces, right axis) and 7 T MCD (black traces, left axis) spectra collected at 4.5 K of (A) free $\text{Co}^{2+}\text{Cbi}^{+}$, (B) $\text{Co}^{2+}\text{Cbi}^{+}$ in the presence of LrPduO , and (C) $\text{Co}^{2+}\text{Cbi}^{+}$ in the presence of the LrPduO/ATP complex. The peak position of the dominant Abs feature (the α -band) is indicated by the solid vertical line.

(Table 2), it causes a small but notable broadening of several features in the 16000–21000 cm^{-1} region of the MCD spectrum. Similarly, the EPR spectrum of $\text{Co}^{2+}\text{Cbi}^{+}$ is slightly perturbed when LrPduO is present, especially between 2800 and 3100 G (cf. panels A and B of Figure 5). Collectively, these data suggest that $\text{Co}^{2+}\text{Cbi}^{+}$ binds to LrPduO even in the absence of cosubstrate ATP but retains a five-coordinate Co^{2+} center with an axially bound water molecule. Interestingly, our simulation of the $\text{Co}^{2+}\text{Cbi}^{+} + \text{LrPduO}$ EPR spectrum reveals that $g_2 \neq g_3$ for this species, indicating that the Co^{2+} ion is in a ligand environment of rhombic symmetry, while for free $\text{Co}^{2+}\text{Cbi}^{+}$, an axially symmetric spectrum where $g_2 = g_3$ is observed (see Table 3).

(B) $\text{Co}^{2+}\text{Cbi}^{+} + \text{LrPduO}/\text{ATP}$. As in the case of $\text{Co}^{2+}\text{Cbl} + \text{LrPduO}/\text{ATP}$ (Figure 2), a significant blue shift of the α -band (Table 2) and the appearance of prominent MCD

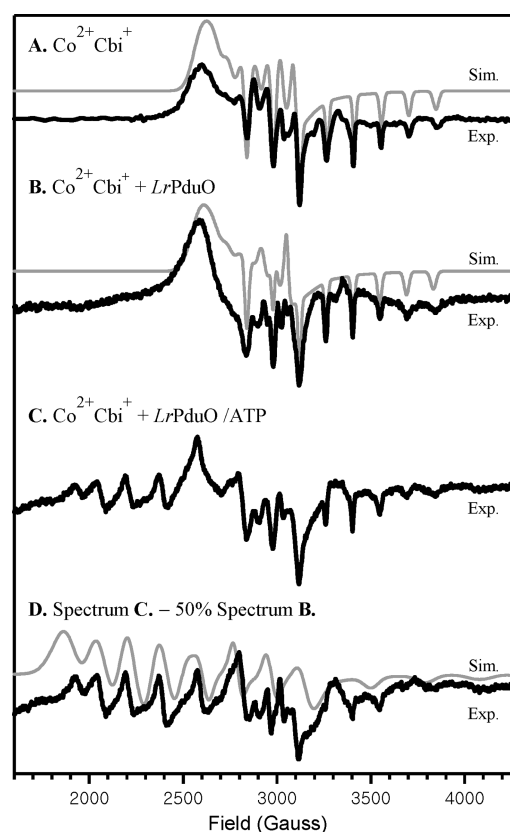


FIGURE 5: EPR spectra collected at 20 K of (A) free $\text{Co}^{2+}\text{Cbi}^{+}$, (B) $\text{Co}^{2+}\text{Cbi}^{+}$ in the presence of LrPduO , and (C) $\text{Co}^{2+}\text{Cbi}^{+}$ in the presence of the LrPduO/ATP complex. Spectrum D was obtained by subtracting 50% of spectrum B from spectrum C. Spectral simulations (thin lines) were performed using the parameters provided in Table 3.

features at 12310 and 20530 cm^{-1} are observed when $\text{Co}^{2+}\text{Cbi}^{+}$ is incubated with LrPduO complexed with the cosubstrate ATP (cf. panels A and C of Figure 4). Again, the conversion to a four-coordinate Co^{2+} corrinoid species is incomplete, based on the observation of weak positive features in the 16000–20000 cm^{-1} region of the $\text{Co}^{2+}\text{Cbl} + \text{LrPduO}/\text{ATP}$ MCD spectrum that are characteristic of five-coordinate $\text{Co}^{2+}\text{Cbi}^{+}$ (Figure 4A).

As anticipated on the basis of our MCD data in Figure 4, the EPR spectrum of $\text{Co}^{2+}\text{Cbi}^{+} + \text{LrPduO}/\text{ATP}$ (Figure 5C) has contributions from two distinct paramagnetic species, an effectively four-coordinate $\text{Co}^{2+}\text{Cbi}^{+}$ species (responsible for the widely spread resonances in the low-field region) and five-coordinate $\text{Co}^{2+}\text{Cbi}^{+}$ possessing an axially bound water molecule (see Figure 5B). To obtain a pure spectrum of the four-coordinate $\text{Co}^{2+}\text{Cbi}^{+}$ fraction, the suitably scaled ($\times 0.5$) $\text{Co}^{2+}\text{Cbi}^{+} + \text{LrPduO}$ EPR spectrum (Figure 5B) was subtracted from the composite spectrum in Figure 5C.

Table 4: Peak Positions of the Prominent MCD Feature in the Near-IR Spectral Region Observed for Co²⁺corrinoids Bound to Several Alkyltransferase–ATP Complexes

Co ²⁺ Cbl + <i>LrPduO</i> /ATP	Co ²⁺ Cbi ⁺ + <i>LrPduO</i> /ATP	Co ²⁺ Cbi ⁺ + CobA/ATP ^a	Co ²⁺ Cbl + hATR/ATP ^b
12340 cm ⁻¹ (810.0 nm)	12310 cm ⁻¹ (812.5 nm)	12340 cm ⁻¹ (810 nm)	12580 cm ⁻¹ (795 nm)

^a From ref 28. ^b From ref 29.

Although the resulting spectrum (Figure 5D) is qualitatively very similar to that exhibited by the four-coordinate Co²⁺Cbl fraction bound to the *LrPduO*/ATP complex (Figure 3D), the g_2 , g_3 , and $A(\text{Co})$ values are in fact somewhat different (Table 3). This result suggests that even though the DMB moiety no longer serves as an axial ligand in the four-coordinate Co²⁺Cbl + *LrPduO*/ATP fraction, it nonetheless modulates the geometric and electronic structures of the Co²⁺ center to a small but noticeable degree, presumably via hydrogen bonding to amino acid residues near the enzyme active site.

DISCUSSION

LrPduO Can Adenosylate Co¹⁺Cbl⁻ and Co¹⁺Cbi. Thus far, only the CobA-type adenosyltransferases were believed to participate in the adenosylation of complete as well as incomplete corrinoids (42). However, the kinetic data obtained in this study provide evidence that in vitro a PduO-type adenosyltransferase can utilize incomplete corrinoids as alternative substrates, in support of a previous proposal that was based on in vivo evidence (32). Interestingly, *LrPduO* adenosylates Co¹⁺Cbl⁻ and Co¹⁺Cbi with approximately the same catalytic efficiency, as judged on the basis of the similar k_{cat}/K_m values (Table 1). Additionally, under saturating ATP conditions, the apparent K_m of *LrPduO* for Co¹⁺Cbi is nearly identical to that reported for Co¹⁺Cbl⁻ and at least 10-fold lower than for any previously reported adenosyltransferase (32). These results suggest that the nucleotide tail (Figure 1) is relatively unimportant for corrinoid binding to the enzyme active site and for product formation. It is important to note, though, that chemically reduced Co¹⁺corrinoids were used in our activity assays. Thus, our kinetic data do not rule out the possibility that the nucleotide tail may be required for allowing the physiological electron donor to accomplish the Co²⁺ → Co¹⁺corrinoid reduction. However, such a requirement is quite unlikely, based on the close resemblance of our spectroscopic data obtained for Co²⁺Cbl and Co²⁺Cbi⁺ bound to the *LrPduO*/ATP complex (see below) and their obvious similarities with those reported for the CobA adenosyltransferase (28).

Interaction between Co²⁺corrinoids and LrPduO in the Absence of Cosubstrate ATP. The fact that the Abs and MCD spectra of Co²⁺Cbl and Co²⁺Cbi⁺ change only slightly when *LrPduO* is added (Figures 2–5) indicates that the geometric and electronic structures of these species are largely preserved in the presence of the enzyme. Nevertheless, small but noticeable changes are observed in each case, signaling that Co²⁺corrinoid binding to the enzyme active site does occur even in the absence of cosubstrate ATP. Specifically, when a solution of Co²⁺Cbl is incubated with *LrPduO*, a significant fraction (~30%) of the cofactor converts to the base-off form, in which the Co²⁺ center is axially ligated by a water molecule instead of the DMB moiety (Figure 1) (35). Alternatively, the addition of *LrPduO* to a solution of

Co²⁺Cbi⁺ causes a small rhombic splitting of the EPR signal (Table 3), possibly reflecting a perturbation of the equatorial ligand environment of the Co²⁺ ion, e.g., via hydrogen bonding of active site residues to the peripheral side chains of the corrin macrocycle.

Interaction between Co²⁺corrinoids and the LrPduO/ATP Complex. While the spectroscopic properties of Co²⁺Cbl and Co²⁺Cbi⁺ are only weakly affected by the addition of *LrPduO*, rather drastic spectral changes were observed when the enzyme was preincubated with the cosubstrate ATP (Figures 2–5). In each case, binding of the Co²⁺corrinoid substrate to the *LrPduO*/ATP complex leads to a substantial blue shift of the dominant Abs feature in the visible spectral region, termed the α -band (Table 2), which corresponds to the lowest-energy corrin-centered $\pi \rightarrow \pi^*$ transition (43–45). Previous studies revealed that the corrin π -based donor orbital involved in this transition also possesses some Co d_{z^2} character, the extent of which is governed by the σ -donor strength of the axial ligand. As a result, the α -band of Co²⁺corrinoids shifts to higher energy with a decrease in electron donating ability of the axial ligand (e.g., from Co²⁺Cbl to Co²⁺Cbi⁺; see Table 2) or a weakening of the axial bonding interaction (35, 46).

The large blue shift of the α -band in response to Co²⁺Cbl and Co²⁺Cbi⁺ binding to the *LrPduO*/ATP complex is accompanied by drastic changes to the corresponding MCD spectra, most notably the appearance of a prominent low-energy feature at ~12340 cm⁻¹ (Figures 2 and 4), as well as to their EPR data, in particular a large increase in the g_2 , g_3 , and $A(\text{Co})$ values (Table 3). Collectively, these spectral perturbations are consistent with a sizable stabilization of the singly occupied Co $3d_{z^2}$ -based molecular orbital (28) because of significant weakening of the axial ligand–Co²⁺corrinoid bonding interaction, generating essentially square-planar Co²⁺ species in the enzyme active site. Although these activated forms of Co²⁺Cbl and Co²⁺Cbi⁺ bound to the *LrPduO*/ATP complex are best described as possessing an effectively four-coordinate Co²⁺ center that lacks any significant axial bonding interactions, the corresponding MCD and EPR spectra (Figures 2–5) exhibit small but notable differences. Specifically, when the alternative substrate Co²⁺Cbi⁺ is used instead of Co²⁺Cbl, the prominent MCD feature in the near-IR spectral region displays a minor red shift [by ~30 cm⁻¹ (Table 4)] and the EPR g and $A(\text{Co})$ values become more rhombic (Table 3). These observations suggest that even though the DMB moiety is displaced from the Co²⁺ ion in the Co²⁺Cbl + *LrPduO*/ATP complex, it may still play a role in organizing the enzyme active site for maximum catalytic activity (e.g., by promoting Co²⁺ → Co¹⁺ reduction).

The spectroscopic data obtained in this work nicely complement the information that has recently been obtained from structural and kinetic studies of *LrPduO*. First, Mera et al. (47) prepared numerous variants of *LrPduO* that were characterized by using kinetic and X-ray crystallographic

techniques to develop a better understanding of the function of several conserved residues in the enzyme active site. Importantly, these studies revealed that substrate inhibition occurs at subsaturating concentrations of ATP, in strong support of an ordered binding scheme according to which the enzyme must bind cosubstrate ATP prior to the corrinoid substrate. Second, in the course of this investigation, St. Maurice et al. (48) succeeded in obtaining an X-ray crystal structure (at 1.9 Å resolution) of Co^{2+}Cbl bound to the *LrPduO*/ATP complex. As expected on the basis of our spectroscopic data reported here, this structure provides visual evidence for the formation of a base-off, four-coordinate Co^{2+}Cbl intermediate in the catalytic cycle of *LrPduO*. This structure also offers clues about how the enzyme imposes such a unique coordination environment on the Co^{2+} corrinoid substrate. Specifically, it shows that the N-terminus of *LrPduO* that is disordered in the substrate-free enzyme (32) becomes ordered upon ATP binding, thereby inducing a distinct active site conformation that is poised for Co^{2+} corrinoid binding (48). Moreover, a conserved Phe residue moves within 3.8 Å of the Co^{2+} ion to promote dissociation of the axially bound solvent ligand that would normally be present in base-off Co^{2+}Cbl . Although not obvious from the *LrPduO* crystal structures, our MCD and EPR data indicate that the formation of such a four-coordinate Co^{2+}Cbl intermediate leads to a significant stabilization of the redox-active $\text{Co } 3d_{z^2}$ orbital that is oriented toward the axial coordination sites, thereby increasing the $\text{Co}^{2+/1+}$ reduction midpoint potential by an estimated 250 mV (28).

Comparison to Other Adenosyltransferases. The involvement of unprecedented, essentially four-coordinate Co^{2+} corrinoid intermediates in the catalytic cycles of adenosyltransferases has originally been proposed on the basis of spectroscopic and computational studies of CobA from *S. enterica* and the human enzyme hATR (28, 29). As expected by taking into consideration the fact that hATR is a PduO-type adenosyltransferase, Co^{2+}Cbl interacts similarly with this enzyme and *LrPduO*. Specifically, while binding of Co^{2+}Cbl to hATR in the absence of ATP leads to a partial (~40%) conversion to the base-off form, a significant blue shift of the α -band and the appearance of the MCD and EPR spectroscopic signatures characteristic of an approximately four-coordinate Co^{2+} corrinoid species are observed when hATR was preincubated with cosubstrate ATP (29). However, the prominent low-energy feature in the MCD spectrum of $\text{Co}^{2+}\text{Cbl} + \text{hATR/ATP}$ is blue-shifted by 240 cm^{-1} relative to that of $\text{Co}^{2+}\text{Cbl} + \text{LrPduO/ATP}$ (Table 4), signifying a slightly stronger residual axial bonding interaction in the former species. Moreover, a comparison of the corresponding EPR spectra reveals that the conversion from the five- to four-coordinate Co^{2+}Cbl species is more complete in the case of hATR (~90%) than for *LrPduO* (~40%). Collectively, these results suggest that a stronger interaction could exist between the dissociated DMB moiety of the activated Co^{2+}Cbl species and the enzyme active site in hATR than in *LrPduO*. It is tempting to speculate, then, that due to this increased level of interaction with the nucleotide loop, hATR may exhibit an increased substrate specificity and thus be unable to adenosylate incompletely assembled corrinoids, such as $\text{Co}^{2+}\text{Cbi}^+$. Although to our knowledge the range of possible corrinoid substrates for hATR has not

yet been established, it is interesting to note that the PduO-type adenosyltransferase from *S. enterica* appears to be specific for AdoCbl synthesis, despite its high degree of similarity in sequence with *LrPduO* (49).

In the case of CobA, for which the natural substrate is a Co^{2+}Cbl precursor that lacks the nucleotide loop and thus more closely resembles $\text{Co}^{2+}\text{Cbi}^+$ (16, 50), MCD and EPR spectroscopic studies revealed that in the $\text{Co}^{2+}\text{Cbi}^+ + \text{CobA/ATP}$ complex, a predominant fraction (~70%) of four-coordinate Co^{2+} corrinoid species is formed (28). When the alternative substrate Co^{2+}Cbl is added to the CobA/ATP complex, however, the conversion to a similar four-coordinate Co^{2+} species is largely suppressed (to ~10%). While hATR and CobA are thus relatively specific for their respective substrates, the results obtained in this study reveal that a sizable fraction of a four-coordinate Co^{2+} corrinoid species is formed regardless of whether Co^{2+}Cbl or $\text{Co}^{2+}\text{Cbi}^+$ binds to the *LrPduO*/ATP complex (40 or 50%, respectively). Although this low substrate specificity of *LrPduO* is consistent with our kinetic data reported in Results and Analysis (Table 1), this finding is rather unexpected, because among the three types of adenosyltransferases found in *S. enterica*, CobA has been presumed to be the only enzyme capable of adenosylating incomplete corrinoid species (7, 8, 16, 28), yet the nearly identical positions of the prominent near-IR features in the MCD spectra of $\text{Co}^{2+}\text{Cbi}^+ + \text{LrPduO/ATP}$ and $\text{Co}^{2+}\text{Cbi}^+ + \text{CobA/ATP}$ (Table 4) suggest that $\text{Co}^{2+}\text{Cbi}^+$ does in fact interact similarly with the *LrPduO*/ATP and CobA/ATP complexes. Despite these similarities, a more complete conversion to a four-coordinate $\text{Co}^{2+}\text{Cbi}^+$ species occurs in the latter enzyme (50 and 70% for *LrPduO* and CobA, respectively).

Although small differences exist among the spectroscopic signatures of the formally four-coordinate Co^{2+} corrinoid species that have now been identified in the active sites of various adenosyltransferases (28, 29), the general strategy of these enzymes evidently involves the formation of an essentially square-planar Co^{2+} corrinoid intermediate, reducing the thermodynamic barrier for the reduction to the Co^{1+} state through stabilization of the redox-active, $\text{Co } 3d_{z^2}$ -based molecular orbital that is oriented along the axial coordination sites of the Co^{2+} ion. Remarkably, for each adenosyltransferase studied to date (28, 29), this activated Co^{2+} corrinoid intermediate is formed in high yield only in the presence of cosubstrate ATP, which provides a mechanism for protecting the enzyme active site from being attacked by the transiently formed Co^{1+} corrinoid “supernucleophile”. Collectively, the insights gained in this study and the recent structural and kinetic characterizations of *LrPduO* provide an excellent basis for further investigations into the fascinating bio-organometallic reaction catalyzed by PduO-type adenosyltransferases.

REFERENCES

1. Butler, P. A., and Kräutler, B. (2006) *Topics in organometallic chemistry*, Vol. 17, Springer Berlin, Heidelberg, Germany.
2. Lenhart, P. G. (1968) The structure of vitamin B₁₂ VII. The X-ray analysis of the vitamin B₁₂ coenzyme. *Proc. R. Soc. London, Ser. A* 303, 45–84.
3. Chowdhury, S., and Banerjee, R. (1999) Role of the dimethylbenzimidazole tail in the reaction catalyzed by coenzyme B₁₂-dependent methylmalonyl-CoA mutase. *Biochemistry* 38, 15287–15294.
4. Banerjee, R. (2001) Radical peregrinations catalyzed by coenzyme B₁₂-dependent enzymes. *Biochemistry* 40, 6191–6198.

5. Chowdhury, S., and Banerjee, R. (2000) Thermodynamic and kinetic characterization of Co–C bond homolysis catalyzed by coenzyme B₁₂-dependent methylmalonyl-CoA mutase. *Biochemistry* 39, 7998–8006.
6. Marsh, E. N. G., and Ballou, D. P. (1998) Coupling of cobalt-carbon bond homolysis and hydrogen atom abstraction in adenosylcobalamin-dependent glutamate mutase. *Biochemistry* 37, 11864–11872.
7. Johnson, C. L. V., Pechonick, E., Park, S. D., Havemann, G. D., Leal, N. A., and Bobik, T. A. (2001) Functional genomic, biochemical, and genetic characterization of the *Salmonella* pduO gene, an ATP:cob(I)alamin adenosyltransferase gene. *J. Bacteriol.* 183, 1577–1584.
8. Buan, N. R., Suh, S.-J., and Escalante-Semerena, J. C. (2004) The eutT gene of *Salmonella enterica* encodes an oxygen-labile, metal-containing ATP:corrinoid adenosyltransferase enzyme. *J. Bacteriol.* 186, 5708–5714.
9. Thoma, N. H., Evans, P. R., and Leadlay, P. F. (2000) Protection of radical intermediates at the active site of adenosylcobalamin-dependent methylmalonyl-CoA mutase. *Biochemistry* 39, 9213–9221.
10. Gerfen, G. J., Licht, S., Willems, J.-P., Hoffman, B. M., and Stubbe, J. (1996) Electron paramagnetic resonance investigations of a kinetically competent intermediate formed in ribonucleotide reduction: Evidence for a thiyl radical-cob(II)alamin interaction. *J. Am. Chem. Soc.* 118, 8192–8197.
11. Brown, K. L., and Zou, X. (1999) Thermolysis of coenzymes B₁₂ at physiological temperatures: Activation parameters for cobalt-carbon bond homolysis and a quantitative analysis of the perturbation of the homolysis equilibrium by the ribonucleoside triphosphate reductase from *Lactobacillus leichmannii*. *J. Inorg. Biochem.* 77, 185–195.
12. Banerjee, R. (2003) Radical carbon skeleton rearrangements: Catalysis by coenzyme B₁₂-dependent mutases. *Chem. Rev.* 103, 2083–2094.
13. Banerjee, R., and Ragsdale, S. W. (2003) The many faces of vitamin B₁₂: Catalysis by cobalamin-dependent enzymes. *Annu. Rev. Biochem.* 72, 209–247.
14. Marsh, E. N. G., and Drennan, C. L. (2001) Adenosylcobalamin-dependent isomerases: New insight into structure and mechanism. *Curr. Opin. Chem. Biol.* 5, 499–505.
15. Fenton, W. A., and Rosenberg, L. E. (1981) The defect in the CblB class of human methylmalonic aciduria: Deficiency of cob(I)alamin adenosyltransferase activity in extracts of cultured fibroblasts. *Biochem. Biophys. Res. Commun.* 98, 283–289.
16. Escalante-Semerena, J. C., Suh, S.-J., and Roth, J. R. (1990) CobA function is required for both de novo cobalamin biosynthesis and assimilation of exogenous corrinoids in *Salmonella typhimurium*. *J. Bacteriol.* 172, 273–280.
17. Dobson, C. M., Wai, T., Leclerc, D., Kadir, H., Narang, M., Lerner-Ellis, J. P., Hudson, T. J., Rosenblatt, D. S., and Gravel, R. A. (2002) Identification of the gene responsible for the cblB complementation group of vitamin B₁₂-dependent methylmalonic aciduria. *Hum. Mol. Genet.* 11, 3361–3369.
18. Warren, M. J., Raux, E., Schubert, H. L., and Escalante-Semerena, J. C. (2002) The biosynthesis of adenosylcobalamin (vitamin B₁₂). *Nat. Prod. Rep.* 19, 390–412.
19. Walker, G. A., Murphy, S., and Huennekens, F. M. (1969) Enzymatic conversion of vitamin B_{12a} to adenosyl-B₁₂: Evidence for the existence of two separate reducing systems. *Arch. Biochem. Biophys.* 134, 95–102.
20. Lawrence, A. D., Deery, E., McLean, K. J., Munro, A. W., Pickersgill, R. W., Rigby, S. E., and Warren, M. J. (2008) Identification, characterization and structure/function analysis of a corrin reductase involved in adenosylcobalamin biosynthesis. *J. Biol. Chem.* 283, 10813–10821.
21. Fonseca, M. V., and Escalante-Semerena, J. C. (2000) Reduction of cob(III)alamin to cob(II)alamin in *Salmonella enterica* Serovar Typhimurium LT2. *J. Bacteriol.* 182, 4304–4309.
22. Olteanu, H., Wolthers, K. R., Munro, A. W., Scrutton, N. S., and Banerjee, R. (2004) Kinetic and thermodynamic characterization of the common polymorphic variants of human methionine synthase reductase. *Biochemistry* 43, 1988–1997.
23. Lexa, D., and Saveant, J.-M. (1983) The electrochemistry of vitamin B₁₂. *Acc. Chem. Res.* 16, 235–243.
24. Mciver, L., Leadbeater, C., Campopiano, D. J., Baxter, R. L., Daff, S. N., Chapman, S. K., and Munro, A. W. (1998) Characterisation of flavodoxin NADP⁺ oxidoreductase and flavodoxin: Key components of electron transfer in *Escherichia coli*. *Eur. J. Biochem.* 257, 557–585.
25. Fonseca, M. V., and Escalante-Semerena, J. C. (2001) An *in vitro* reducing system for the enzymic conversion of cobalamin to adenosylcobalamin. *J. Biol. Chem.* 276, 32101–32108.
26. Sampson, E. M., Johnson, C. L. V., and Bobik, T. A. (2005) Biochemical evidence that the pduS gene encodes a bifunctional cobalamin reductase. *Microbiology* 151, 1169–1177.
27. Leal, N. A., Olteanu, H., Banerjee, R., and Bobik, T. A. (2004) Human ATP:cob(I)alamin adenosyltransferase and its interaction with methionine synthase reductase. *J. Biol. Chem.* 279, 47536–47542.
28. Stich, T. A., Buan, N. R., Escalante-Semerena, J. C., and Brunold, T. C. (2005) Spectroscopic and computational studies of the ATP:corrinoid adenosyltransferase (CobA) from *Salmonella enterica*: Insights into the mechanism of adenosylcobalamin biosynthesis. *J. Am. Chem. Soc.* 127, 8710–8719.
29. Stich, T. A., Yamanishi, M., Banerjee, R., and Brunold, T. C. (2005) Spectroscopic evidence for the formation of a four-coordinate Co²⁺cobalamin species upon binding to the human ATP:cobalamin adenosyltransferase. *J. Am. Chem. Soc.* 127, 7660–7661.
30. Leal, N. A., Park, S. D., Kima, P. E., and Bobik, T. A. (2003) Identification of the human and bovine ATP:cob(I)alamin adenosyltransferase cDNAs based on complementation of a bacterial mutant. *J. Biol. Chem.* 278, 9227–9234.
31. Dobson, C. M., Wai, T., Leclerc, D., Wilson, A., Wu, X., Dore, C., Hudson, T., Rosenblatt, D. S., and Gravel, R. A. (2002) Identification of the gene responsible for the cblA complementation group of vitamin B₁₂-responsive methylmalonic aciduria based on analysis of prokaryotic gene arrangements. *Proc. Natl. Acad. Sci. U.S.A.* 99, 15554–15559.
32. St. Maurice, M., Mera, P. E., Taranto, M. P., Sesma, F., Escalante-Semerena, J. C., and Rayment, I. (2007) Structural characterization of the active site of the PduO-type ATP:co(I)rrinoid adenosyltransferase from *Lactobacillus reuteri*. *J. Biol. Chem.* 282, 2596–2605.
33. Rocco, C. J., Dennison, K. L., Klenchin, V. A., Rayment, I., and Escalante-Semerena, J. C. (2008) Construction and use of new cloning vectors for the rapid isolation of recombinant proteins from *Escherichia coli*. *Plasmid* XXX–XXX. (in press).
34. Neese, F. (1997) Electronic Structure and Spectroscopy of Novel Copper Chromophores in Biology, Ph.D. Thesis, University of Konstanz, Konstanz, Germany.
35. Stich, T. A., Buan, N. R., and Brunold, T. C. (2004) Spectroscopic and computational studies of Co²⁺corrinoids: Spectral and electronic properties of the biologically relevant base-on and base-off forms of Co²⁺cobalamin. *J. Am. Chem. Soc.* 126, 9735–9749.
36. Pilbrow, J. R. (1982) in B₁₂ (Dolphin, D., Ed.) pp 431–462, Wiley, New York.
37. Doorslaer, S. V., Jeschke, G., Epel, B., Goldfarb, D., Eichel, R.-A., Kräutler, B., and Schweiger, A. (2003) Axial solvent coordination in “base-off” cob(II)alamin and related Co(II)-corrinates revealed by 2D-EPR. *J. Am. Chem. Soc.* 125, 5915–5927.
38. Johnson, M. K. (2000) in *Physical methods in bioinorganic chemistry* (Que, L., Jr., Ed.) pp 233–285, University Science Books, Sausalito, CA.
39. Schellman, J. A. (1975) Circular dichroism and optical rotation. *Chem. Rev.* 75, 323–331.
40. Ozarowski, A., Lee, H. M., and Balch, A. L. (2003) Crystal environments probed by EPR spectroscopy. Variations in the EPR spectra of Co^{II}(octaethylporphyrin) doped in crystalline diamagnetic hosts and a reassessment of the electronic structure of four-coordinate cobalt(II). *J. Am. Chem. Soc.* 125, 12606–12614.
41. Assour, J. M., and Kahn, W. K. (1965) Electron spin resonance of α - and β -cobalt phthalocyanine. *J. Am. Chem. Soc.* 87, 207–212.
42. Suh, S.-J., and Escalante-Semerena, J. C. (1995) Purification and initial characterization of the ATP:corrinoid adenosyltransferase encoded by the cobA gene of *Salmonella typhimurium*. *J. Bacteriol.* 177, 921–925.
43. Kuhn, H., Drexhage, K. H., and Martin, H. (1965) The light absorption of vitamin B₁₂. *Proc. R. Soc. London, Ser. A* 288, 348–351.
44. Firth, R. A., Hill, H. A. O., Pratt, J. M., Williams, R. J. P., and Jackson, W. R. (1967) The circular dichroism and absorption spectra of some vitamin B₁₂ derivatives. *Biochemistry* 6, 2178–2189.
45. Day, P. (1967) A theory of the optical properties of vitamin B₁₂ and its derivatives. *Theor. Chim. Acta* 7, 328–341.

46. Stich, T. A., Brooks, A. J., Buan, N. R., and Brunold, T. C. (2003) Spectroscopic and computational studies of Co^{3+} -corrinoids: Spectral and electronic properties of the B_{12} cofactors and biologically relevant precursors. *J. Am. Chem. Soc.* 125, 5897–5914.
47. Mera, P. E., St. Maurice, M., Rayment, I., and Escalante-Semerena, J. C. (2007) Structural and functional analyses of the human-type corrinoid adenosyltransferase (PduO) from *Lactobacillus reuteri*. *Biochemistry* 46, 13829–13836.
48. St. Maurice, M., Mera, P. E., Park, K., Brunold, T. C., Escalante-Semerena, J. C., and Rayment, I. (2008) Structural characterization of a human-type corrinoid adenosyltransferase confirms that coenzyme B_{12} is synthesized through a four-coordinate intermediate. *Biochemistry* 47, 5755–5766.
49. Johnson, C. L., Pechonick, E., Park, S. D., Havemann, G. D., Leal, N. A., and Bobik, T. A. (2001) Functional genomic, biochemical, and genetic characterization of the *Salmonella pduO* gene, an ATP: cob(I)alamin adenosyltransferase gene. *J. Bacteriol.* 183, 1577–1584.
50. O'Toole, G. A., and Escalante-Semerena, J. C. (1993) cobU-dependent assimilation of nonadenosylated cobinamide in cobA mutants of *Salmonella typhimurium*. *J. Bacteriol.* 175, 6328–6336.

BI800419E